Circularly polarized soft x-ray diffraction study of helical magnetism in hexaferrite

A. M. Mulders,[1,2] S. M. Lawrence,[1] A. J. Princep,[1] U. Staub,[3] Y. Bodenthin,[3] M. García-Fernández,[3] M. Garganourakis,[3] J. Hester,[2] R. Macquart,[4] and C. D. Ling[2,4]

[1]*Department of Imaging and Applied Physics, Curtin University of Technology, Perth, Western Australia 6845, Australia*

[2]*The Bragg Institute, Australian Nuclear Science and Technology Organisation, Lucas Heights, New South Wales 2234, Australia*

[3]*Swiss Light Source, Paul Scherrer Institut, 5232 Villigen PSI, Switzerland*

[4]*School of Chemistry, The University of Sydney, Sydney, New South Wales 2006, Australia*

(Received 20 November 2009; revised manuscript received 20 January 2010; published 26 March 2010)

Magnetic spiral structures can exhibit ferroelectric moments as recently demonstrated in various multiferroic materials. In such cases the helicity of the magnetic spiral is directly correlated with the direction of the ferroelectric moment and measurement of the helicity of magnetic structures is of current interest. Soft x-ray resonant diffraction is particularly advantageous because it combines element selectivity with a large magnetic cross-section. We calculate the polarization dependence of the resonant magnetic x-ray cross-section (electric dipole transition) for the basal plane magnetic spiral in hexaferrite $Ba_{0.8}Sr_{1.2}Zn_2Fe_{12}O_{22}$ and deduce its domain population using circular polarized incident radiation. We demonstrate there is a direct correlation between the diffracted radiation and the helicity of the magnetic spiral.

DOI: 10.1103/PhysRevB.81.092405 PACS number(s): 75.25.-j, 61.05.cc, 75.50.Dd, 75.85.+t

Magnetic spiral structures can exhibit ferroelectric moments as recently demonstrated in various multiferroic materials.[1–4] In such cases the helicity of the magnetic spiral is directly correlated with the direction of the ferroelectric moment and measurement of the helicity of magnetic structures is of current interest. Magnetic spiral structures have been observed directly with neutron diffraction (ND) and resonant x-ray diffraction (RXD)[5] as their superstructure gives rise to satellite reflections. With polarized neutron diffraction the chirality of the magnetic structure can be determined, as was first predicted by Blume[6] and achieved by Siratori.[7] Recently this has been particularly insightful for the study of ferroelectric magnetic spiral structures in $TbMnO_3$,[8] $LiCu_2O_2$,[9] and $CuFe_{1-x}Al_xO_2$[10] observing that the chirality of the magnetic structure is manipulated with applied electric field. With circular polarized nonresonant x-ray diffraction the chiral magnetic domain population in holmium has been determined[11] and, very recently, polarization analysis has been used to study the cycloidal magnetic domains in multiferroic $TbMnO_3$ in its ferroelectric phase.[12]

An advantage of RXD is that via tuning the incident energy to a particular absorption edge, element specific magnetism is observed. In the case of transition metals, the $L_{2,3}$ edge is particularly insightful because the core electron is excited from the core $2p$ to the $3d$ valence states and the (empty) magnetic states are directly probed. The magnetic cross-section is significant compared to the charge cross-section and soft x-ray resonant diffraction has emerged as a very valuable technique with which to study magnetic and orbital order in transition-metal oxides, in particular to distinguish between charge, orbital, and magnetic order.[13–16] Correlation between the RXD intensity and the helicity of the magnetic spiral has been demonstrated by imaging of the spiral domains in holmium[17] but a quantitative analysis of the diffracted intensities is missing.

In this Brief Report we calculate the polarization dependence of the RXD cross-section and deduce the domain population of the magnetic spiral structure in hexaferrite using variably polarized incident radiation at the Fe L_3 edge ($\lambda = 17.45$ Å). We demonstrate that XRD is well suited to study magnetoelectric coupling in multiferroic materials that exhibit magnetic spiral components.

The helical magnetic structure of $Ba_{0.5}Sr_{1.5}Zn_2Fe_{12}O_{22}$ hexaferrite[18] has been studied with neutron scattering[19–21] and polarized x-ray diffraction[22] and is characterized by $(0\ 0\ l^{\pm})$ satellites with $l^{\pm} = 3n \pm 3\tau$. Competition among superexchange interactions leads to a distorted helimagnetic structure consisting of large and small ferrimagnetic bunches with moments aligned in the *ab* plane and modulation wave vector $(0\ 0\ \tau)$. Electric polarization arises under applied magnetic field in the intermediate-III magnetic phase, characterized by $\tau = 0.5$.

Hexaferrite single crystals were grown in a manner similar to that given by Momozawa *et al.*[23] Reactants were mixed in the molar ratio 4.92% $BaCO_3$, 14.77% $SrCO_3$, 19.69% ZnO, 53.61% Fe_2O_3, and 7.01% Na_2CO_3 flux and heated in a Pt crucible to 1420 °C at a rate of 20 °C/min and left there for 20 h. Rapid temperature cycling[23] was employed to remove impurity crystals followed by slow cooling (0.2 °C/h) between 1185 and 1155 °C to improve crystal size.

Elemental analysis with inductively coupled plasma atomic emission spectroscopy gave a stoichiometry of $Ba_{0.8}Sr_{1.2}Zn_2Fe_{12}O_{22}$, with small variations in Ba/Sr ratio depending on the single crystal. Magnetization measurements were performed with a Quantum Design 7T MPMS at the magnetics laboratory at the University of Western Australia. The single crystals exhibited consecutive magnetization steps as function of applied magnetic field in the *ab* plane, similar to results reported earlier.[4,20] Single-crystal neutron diffraction was performed at the Wombat diffractometer at OPAL with $\lambda = 2.955$ Å and showed temperature-dependent incommensurate τ for $B = 0$ T, $\tau = 0.5$ for $0.5 \leq B \leq 2.0$ T, and $\tau = 1$ for $B \geq 2.25$ T (at $T = 100$ K). Soft x-ray resonant diffraction was performed at the RESOXS end station of the SIM beamline at the Swiss Light Source of the Paul Scherrer Institut.[24] The elliptical twin undulator UE56 (Apple II) of the beamline can produce variable linear and circular polarization. The hexaferrite sample was mounted with the *c* axis

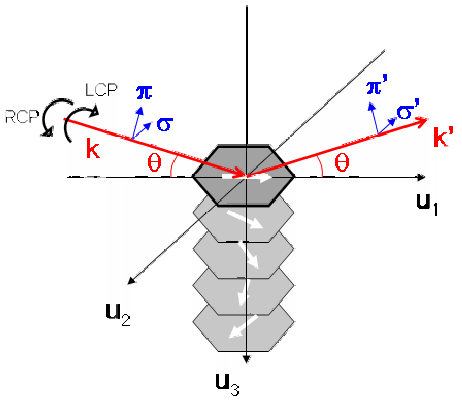

FIG. 1. (Color online) Experimental setup with coordinate system used for calculating the polarization-dependent resonant cross-section. The basal plane magnetic spiral with helicity S^+ is indicated.

in the scattering plane and the a axis perpendicular to the scattering plane (see Fig. 1) and its temperature was regulated between 15 and 325 K.

X-ray diffraction from magnetic spiral structures gives rise to satellite reflections, which have polarization-dependent magnetic scattering cross-sections.[25] The intensity from magnetic moments is proportional to $(\hbar\omega/mc^2)^2$ and is generally weak. However, this is enhanced by orders of magnitude when the x-ray energy is tuned to an absorption edge that excites a core electron to the empty valence states. In case of transition metals this is the L_3 edge (electric dipole transition) and the resonant magnetic scattering amplitude of the magnetic satellites equals[5]

$$f_{\varepsilon'\varepsilon}^{XRES} = -\frac{3}{4k} i(\hat{\varepsilon}' \times \hat{\varepsilon}) \cdot \hat{\mathbf{z}}_j [F_{11} - F_{1-1}], \tag{1}$$

where $\boldsymbol{\varepsilon}$ and $\boldsymbol{\varepsilon}'$ are the polarization of the incident and diffracted radiations, $\hat{\mathbf{z}}_j$ the quantization axis of the magnetic moment at atom j and F_{11}, F_{1-1} are the atomic properties of the initial and excited states of the Fe ion which is related to the $3d$ magnetic moment and the overlap integral. $\mathbf{q}=\mathbf{k}-\mathbf{k}'$ is the wave-vector transfer and $\mathbf{k}$ and $\mathbf{k}'$ are the wave vectors of the incident and diffracted radiations, respectively. The sum over magnetic ions j gives the magnetic structure factor $M_{\varepsilon'\varepsilon}^{XRES} = \Sigma_j \exp(i\mathbf{q}\cdot\mathbf{r}_j) f_{\varepsilon'\varepsilon}^{XRES}$.

Hill and McMorrow[26] have formulated the resonant x-ray cross-section in terms of linear polarized radiation. Recently, Lovesey *et al.*[27] formulated the resonant diffracted intensity for circular polarized radiation in terms of the scattering factors for linear polarization. Without polarization analysis the diffracted intensities I_ε^{XRES} equal

$$I_\sigma^{XRES} = |M_{\sigma'\sigma}|^2 + |M_{\pi'\sigma}|^2, \tag{2}$$

$$I_\pi^{XRES} = |M_{\sigma'\pi}|^2 + |M_{\pi'\pi}|^2, \tag{3}$$

$$I_\chi^{XRES} = \frac{1}{2}(|M_{\sigma'\sigma}|^2 + |M_{\pi'\sigma}|^2 + |M_{\sigma'\pi}|^2 + |M_{\pi'\pi}|^2) + \chi \,\mathrm{Im}\{M_{\sigma'\sigma} M_{\sigma'\pi}^* + M_{\pi'\sigma} M_{\pi'\pi}^*\}, \tag{4}$$

where π polarization is parallel to the scattering plane and σ polarization is perpendicular to the scattering plane (see Fig. 1). $\chi=+1$ indicates right circular polarized (RCP) and $\chi=-1$ left circular polarized (LCP) of the incident beam. The last term of Eq. (4) generally vanishes but can be nonzero as demonstrated for the case of the enantiomorphic screw axis in quartz.[28]

We approximate the magnetic structure of hexaferrite with a single magnetic moment that rotates either clockwise (positive helicity S^+) or anticlockwise (negative helicity S^-) for consecutive atoms along the c axis. For a basal plane magnetic spiral with modulation wave vector $(0\ 0\ \tau)$ the moment direction for S^+ and S^- equals $\hat{\mathbf{z}}_j^{\pm} = \hat{\mathbf{u}}_1 \cos(\boldsymbol{\tau}\cdot\mathbf{r}_j) \pm \hat{\mathbf{u}}_2 \sin(\boldsymbol{\tau}\cdot\mathbf{r}_j) = \frac{1}{2}[\hat{\mathbf{u}}_\mp \exp(i\boldsymbol{\tau}\cdot\mathbf{r}_j) + \hat{\mathbf{u}}_\pm \exp(-i\boldsymbol{\tau}\cdot\mathbf{r}_j)]$ with $\hat{\mathbf{u}}_\pm = \hat{\mathbf{u}}_1 \pm i\hat{\mathbf{u}}_2$. The unit vectors $\hat{\mathbf{u}}_1$, $\hat{\mathbf{u}}_2$, and $\hat{\mathbf{u}}_3$ define the coordinate system with respect to the diffraction plane. $\hat{\mathbf{u}}_1$ is parallel to $\mathbf{k}'+\mathbf{k}$, $\hat{\mathbf{u}}_2$ is perpendicular to the scattering plane, and $\hat{\mathbf{u}}_3$ is parallel to $\mathbf{k}'-\mathbf{k}$ (see Fig. 1). In this experiment the c axis of hexaferrite is aligned along $\hat{\mathbf{u}}_3$. The cross terms of polarization $\hat{\varepsilon}' \times \hat{\varepsilon}$ in Eq. (1) equal $\boldsymbol{\sigma}' \times \boldsymbol{\sigma} = 0$, $\boldsymbol{\sigma}' \times \boldsymbol{\pi} = \hat{\mathbf{k}}$, $\boldsymbol{\pi}' \times \boldsymbol{\sigma} = -\hat{\mathbf{k}}'$, and $\boldsymbol{\pi}' \times \boldsymbol{\pi} = \hat{\mathbf{k}}' \times \hat{\mathbf{k}}$. Consequently, the polarization-dependent magnetic structure factors are

$$M_{\sigma'\sigma} = 0, \tag{5}$$

$$M_{\pi'\sigma} = -\frac{3}{4k} i \sum_j (-\hat{\mathbf{k}}' \cdot \hat{\mathbf{z}}_j^{\pm})[F_{11} - F_{1-1}] \exp(i\mathbf{q}\cdot\mathbf{r}_j), \tag{6}$$

$$M_{\sigma'\pi} = -\frac{3}{4k} i \sum_j (\hat{\mathbf{k}} \cdot \hat{\mathbf{z}}_j^{\pm})[F_{11} - F_{1-1}] \exp(i\mathbf{q}\cdot\mathbf{r}_j), \tag{7}$$

$$M_{\pi'\pi} = -\frac{3}{4k} i \sum_j (\hat{\mathbf{k}}' \times \hat{\mathbf{k}}) \cdot \hat{\mathbf{z}}_j^{\pm} [F_{11} - F_{1-1}] \exp(i\mathbf{q}\cdot\mathbf{r}_j). \tag{8}$$

Using $\hat{\mathbf{k}} = \hat{\mathbf{u}}_1 \cos\theta + \hat{\mathbf{u}}_3 \sin\theta$, $\hat{\mathbf{k}}' = \hat{\mathbf{u}}_1 \cos\theta - \hat{\mathbf{u}}_3 \sin\theta$, and $\hat{\mathbf{k}}' \times \hat{\mathbf{k}} = -\hat{\mathbf{u}}_2 \sin 2\theta$ gives for the resonant intensity of the magnetic satellites

$$I_{\sigma,S^\pm}^{XRES} \propto \cos^2\theta [F_{11} - F_{1-1}] \delta(\mathbf{q} \pm \boldsymbol{\tau}), \tag{9}$$

$$I_{\pi,S^\pm}^{XRES} \propto (\cos^2\theta + \sin^2 2\theta)[F_{11} - F_{1-1}] \delta(\mathbf{q} \pm \boldsymbol{\tau}), \tag{10}$$

$$I_{\chi,S^+}^{XRES} \propto \left(\cos^2\theta + \frac{1}{2}\sin^2 2\theta \mp \chi \cos\theta \sin 2\theta\right) \times [F_{11} - F_{1-1}]^2 \delta(\mathbf{q} \pm \boldsymbol{\tau}), \tag{11}$$

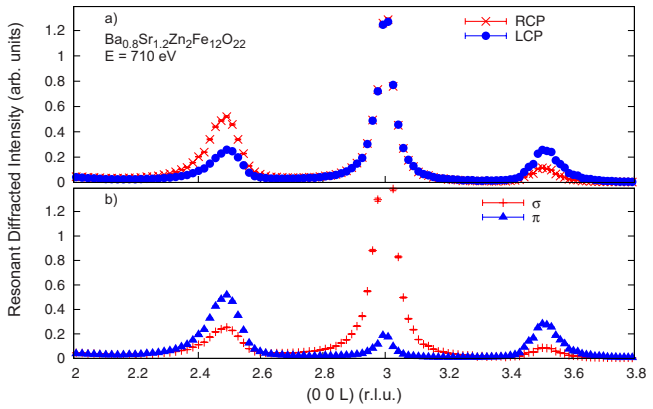

FIG. 2. (Color online) Resonant diffraction of hexaferrite at $T=35$ K recorded with (a) circular- and (b) linear-polarized incident radiations at the Fe L_3 edge. Note the asymmetry in intensity of the two magnetic satellites neighboring the (003) reflection recorded with RCP (red crosses) and LCP (blue filled spheres). σ (blue filled triangles) and π (red plusses) diffractions do not distinguish between positive and negative helicities of the magnetic spiral.

$$I_{\chi,S^-}^{XRES} \propto \left(\cos^2\theta + \frac{1}{2}\sin^2 2\theta \pm \chi \cos\theta \sin 2\theta\right) \times [F_{11} - F_{1-1}]^2 \delta(\mathbf{q} \pm \boldsymbol{\tau}). \quad (12)$$

The diffracted intensity for linear polarization is independent of the helicity of the magnetic spiral, in contrast to the diffracted intensity for circular polarization, which is distinct for S^+ and S^-. The term proportional to $\cos\theta \sin 2\theta$ is opposite in sign for the satellites at $(0\ 0\ l^-)$ and $(0\ 0\ l^+)$ and, for each satellite, the difference in resonant intensity for RCP and LCP incident radiation is proportional to $2\cos\theta \sin 2\theta [F_{11} - F_{1-1}]^2$. This demonstrates a direct correlation between diffracted intensity of circularly polarized x rays and the helicity of the magnetic spiral. The deduced intensities [Eqs. (9)–(12)] are independent of rotation of the sample around the scattering factor $\mathbf{q}$.

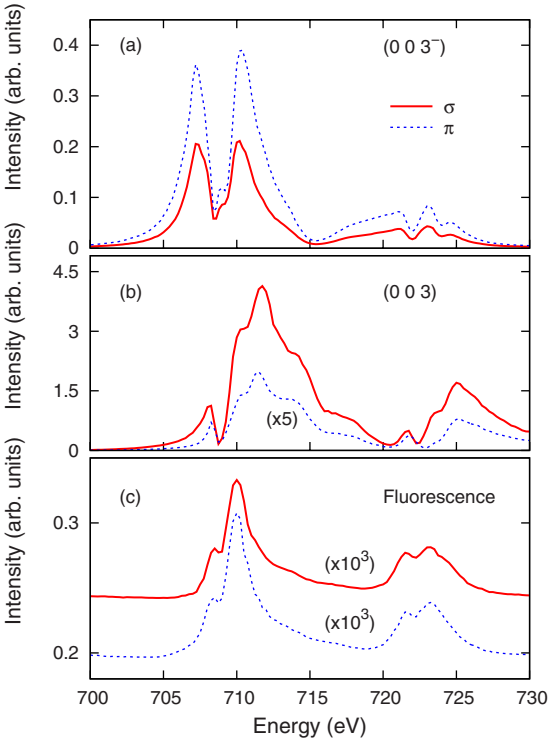

FIG. 3. (Color online) (a) Energy dependence of the (003^-) magnetic satellite (b) compared to the (003) structural reflection and (c) the fluorescence yield, recorded with σ (solid red) and π (dotted blue) linear polarized incident radiations. Note the scaling factors used. The spectra were recorded at $T \sim 90$ K, 132 K, and 138 K, respectively, and are not corrected for absorption.

TABLE I. Experimental (exp.) and calculated (calc.) intensities for the magnetic satellites observed in hexaferrite using 77% of magnetic domains with S^+ and 23% of magnetic domains with S^-. A single scaling factor was used between experimental and calculated intensities.

	(003^-)		(003^+)	
Incident polarization	Exp.	Calc.	Exp.	Calc.
RCP	0.50	0.52	0.11	0.10
LCP	0.24	0.25	0.25	0.23
σ	0.23	0.26	0.08	0.08
π	0.50	0.51	0.27	0.25

Figure 2 illustrates that $(0\ 0\ 3^+)$ is most intense for LCP and $(0\ 0\ 3^-)$ is most intense for RCP radiation. In contrast, linear polarization of the incident radiation does not result in such asymmetry. The diffracted intensity for π radiation is stronger than for σ radiation consistent with Eqs. (9) and (10). The resonant Bragg intensity as a function of incident energy for the $(003^{\pm})$ satellite is distinct from that of the (003) reflection and orders of magnitude stronger than the fluorescence yield (Fig. 3). Table I compares the observed and calculated intensities demonstrating good agreement, 77% exhibits a magnetic spiral with S^- and 23% a magnetic

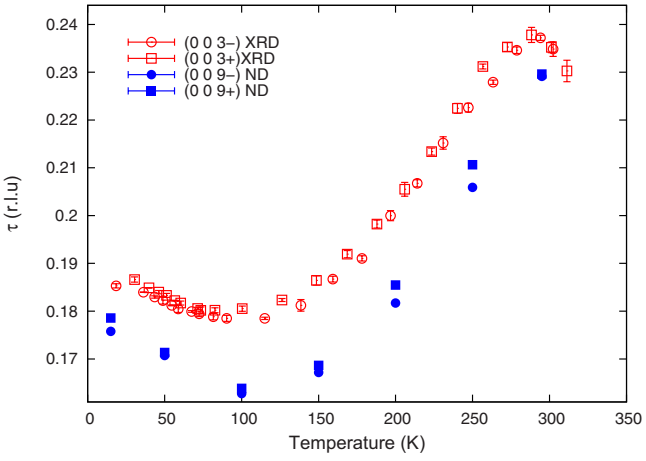

FIG. 4. (Color online) Wave vector of the magnetic spiral in hexaferrite as a function of temperature deduced from the resonant magnetic satellite diffraction (open symbols) and neutron diffraction (solid symbols). The difference in the magnitude of τ for XRD and ND is attributed to stoichiometry variation between the single crystals used in the experiments.

spiral with S^+ within the illuminated sample area of ~ 1 mm^2.

Figure 4 shows the gradual modulation of the wave vector of the magnetic spiral with increasing temperature. Variations in stoichiometry result in different τ due to modification of the superexchange interaction. The general trend is similar to that observed for $Ba_{0.5}Sr_{1.5}Zn_2Fe_{12}O_{22}$.[19,21]

RXD from the magnetic spiral is intense and on average about a factor of two smaller than the diffracted intensity at (003). This is much stronger than the nonresonant x-ray diffracted intensity reported for $Ba_{0.5}Sr_{1.5}Zn_2Fe_{12}O_{22}$.[22] The long wavelength makes soft x-ray resonant diffraction particularly suited to study magnetic structures with large periodicity. Recently, soft x-ray diffraction studies at the Mn L_3 edge have measured the magnetic spin structure and order parameter in multiferroic $TbMn_2O_5$ demonstrating the magnetoelectric effect arises from noncollinear spin moments.[29] An *in situ* applied electric field demonstrated significant manipulation and the excitation of commensurate magnetic order in multiferroic $ErMn_2O_5$.[30] Very recently circularly polarized radiation at the Dy M_5 resonance has been used to write and read chiral domains in multiferroic $DyMnO_3$.[31]

In summary, we present polarization-dependent resonant diffraction cross-sections for σ, π, LCP, and RCP incident radiation and determine the spiral magnetic domain population. This demonstrates the potential of using circular polarized soft x-ray resonant diffraction for investigation of long-wavelength magnetic structures. Compared to polarized neutron studies, this method records element specific magnetic helicity and allows to differentiate between distinct magnetic ions within one material. The large diffracted intensity, limited sample size requirements, and speed of collection times are an additional advantage.

We acknowledge discussion with Hoyoung Jang. This work was partly performed at the SLS of the Paul Scherrer Institut, Villigen, Switzerland. We thank the beamline staff of X11MA and Robert Woodward from UWA for their support. We acknowledge financial support from the Swiss National Science Foundation, AINSE, Access to Major Research Facilities Programme, and the ARC-Discovery Projects (Grants No. DP0666465).

[1] T. Kimura, T. Goto, H. Shintani, K. Ishizaka, T. Arima, and Y. Tokura, Nature (London) **426**, 55 (2003).
[2] K. Taniguchi, N. Abe, T. Takenobu, Y. Iwasa, and T. Arima, Phys. Rev. Lett. **97**, 097203 (2006).
[3] G. Lawes, A. B. Harris, T. Kimura, N. Rogado, R. J. Cava, A. Aharony, O. Entin-Wohlman, T. Yildrim, M. Kenzelmann, C. Broholm, and A. P. Ramirez, Phys. Rev. Lett. **95**, 087205 (2005).
[4] T. Kimura, G. Lawes, and A. P. Ramirez, Phys. Rev. Lett. **94**, 137201 (2005).
[5] J. P. Hannon, G. T. Trammell, M. Blume, and D. Gibbs, Phys. Rev. Lett. **61**, 1245 (1988).
[6] M. Blume, Phys. Rev. **130**, 1670 (1963).
[7] K. Siratori, J. Akimitsu, E. Kita, and M. Nishi, J. Phys. Soc. Jpn. **48**, 1111 (1980).
[8] Y. Yamasaki, H. Sagayama, T. Goto, M. Matsuura, K. Hirota, T. Arima, and Y. Tokura, Phys. Rev. Lett. **98**, 147204 (2007).
[9] S. Seki, Y. Yamasaki, M. Soda, M. Matsuura, K. Hirota, and Y. Tokura, Phys. Rev. Lett. **100**, 127201 (2008).
[10] T. Nakajima, S. Mitsuda, S. Kanetsuki, K. Tanaka, K. Fujii, N. Terada, M. Soda, M. Matsuura, and K. Hirota, Phys. Rev. B **77**, 052401 (2008).
[11] C. Sutter, G. Grübel, C. Vettier, F. de Bergevin, A. Stunault, D. Gibbs, and C. Giles, Phys. Rev. B **55**, 954 (1997).
[12] F. Fabrizi, H. C. Walker, L. Paolasini, F. de Bergevin, A. T. Boothroyd, D. Prabhakaran, and D. F. McMorrow, Phys. Rev. Lett. **102**, 237205 (2009).
[13] U. Staub, V. Scagnoli, A. M. Mulders, K. Katsumata, Z. Honda, H. Grimmer, M. Horisberger, and J. M. Tonnerre, Phys. Rev. B **71**, 214421 (2005).
[14] S. B. Wilkins, N. Stojic, T. A. W. Beale, N. Binggeli, C. W. M. Castleton, P. Bencok, D. Prabhakaran, A. T. Boothroyd, P. D. Hatton, and M. Altarelli, Phys. Rev. B **71**, 245102 (2005).
[15] J. Herrero-Martín, J. Garcia, G. Subías, J. Blasco, M. C. Sánchez, and S. Stanescu, Phys. Rev. B **73**, 224407 (2006).
[16] V. Scagnoli, U. Staub, A. M. Mulders, M. Janousch, G. I. Meijer, G. Hammerl, J. M. Tonnerre, and N. Stojic, Phys. Rev. B **73**, 100409(R) (2006).
[17] J. C. Lang, D. R. Lee, D. Haskel, and G. Srajer, J. Appl. Phys. **95**, 6537 (2004).
[18] U. Enz, J. Appl. Phys. **32**, 22S (1961).
[19] N. Momozawa, J. Phys. Soc. Jpn. **55**, 4007 (1986).
[20] N. Momozawa and Y. Yamaguchi, J. Phys. Soc. Jpn. **62**, 1292 (1993).
[21] S. Utsumi, D. Yoshiba, and N. Momozawa, J. Phys. Soc. Jpn. **76**, 034704 (2007).
[22] E. Tsuji, T. Kurasawa, I. Yazawa, H. Katoh, N. Momozawa, K. Ishida, and S. Kishimoto, J. Phys. Soc. Jpn. **65**, 610 (1996).
[23] N. Momozawa, H. Takei, and M. Mita, J. Cryst. Growth **83**, 403 (1987).
[24] U. Staub, V. Scagnoli, Y. Bodenthin, M. García-Fernández, R. Wetter, A. M. Mulders, H. Grimmer, and M. Horisberger, J. Synchrotron Radiat. **15**, 469 (2008).
[25] M. Blume and D. Gibbs, Phys. Rev. B **37**, 1779 (1988).
[26] J. P. Hill and D. F. McMorrow, Acta Crystallogr., Sect. A: Found. Crystallogr. **52**, 236 (1996).
[27] S. W. Lovesey, E. Balcar, and Y. Tanaka, J. Phys.: Condens. Matter **20**, 272201 (2008).
[28] Y. Tanaka, T. Takeuchi, S. W. Lovesey, K. S. Knight, A. Chainani, Y. Takata, M. Oura, Y. Senba, H. Ohashi, and S. Shin, Phys. Rev. Lett. **100**, 145502 (2008).
[29] J. Okamoto, D. J. Huang, C. Y. Mou, K. S. Chao, H. J. Lin, S. Park, S.-W. Cheong, and C. T. Chen, Phys. Rev. Lett. **98**, 157202 (2007).
[30] Y. Bodenthin, U. Staub, M. García-Fernández, M. Janoschek, J. Schlappa, E. I. Golovenchits, V. A. Sanina, and S. G. Lushnikov, Phys. Rev. Lett. **100**, 027201 (2008).
[31] E. Schierle, V. Soltwisch, D. Schmitz, R. Feyerherm, A. Maljuk, F. Yokaichiya, D. N. Argyriou, and E. Weschke, arXiv:0910.5663 (unpublished).